Hindawi Publishing Corporation
Shock and Vibration
Volume 2016, Article ID 5121932, 10 pages
http://dx.doi.org/10.1155/2016/5121932

Research Article

Study on Impact Damage and Energy Dissipation of Coal Rock Exposed to High Temperatures

Tu-bing Yin,[1,2] Kang Peng,[1,3] Liang Wang,[1,3] Pin Wang,[2] Xu-yan Yin,[3] and Yong-liang Zhang[4]

[1]*State Key Laboratory of Coal Mine Disaster Dynamics and Control, Chongqing University, Chongqing 400044, China*
[2]*School of Resources and Safety Engineering, Central South University, Changsha 410083, China*
[3]*College of Resources and Environmental Science, Chongqing University, Chongqing 400030, China*
[4]*Automotive School, Qingdao Technological University, Qingdao, Shandong 266520, China*

Correspondence should be addressed to Kang Peng; pengkang@cqu.edu.cn

Received 8 June 2016; Accepted 15 September 2016

Academic Editor: M. I. Herreros

The dynamic failure characteristics of coal rock exposed to high temperatures were studied by using a split Hopkinson pressure bar (SHPB) system. The relationship between energy and time history under different temperature conditions was obtained. The energy evolution and the failure modes of specimens were analyzed. Results are as follows: during the test, more than 60% of the incident energy was not involved in the breaking of the sample, while it was reflected back. With the increase of temperature, the reflected energy increased continuously; transmitted and absorbed energy showed an opposite variation. At the temperature of 25 to 100°C, the absorbed energy was less than that transmitted, while this phenomenon was opposite after 100°C. The values of specific energy absorption (SEA) were distributed at 0.04 to 0.1 J·cm^{-3}, and its evolution with temperature could be divided into four different stages. Under different temperature conditions, the failure modes and the broken blocks of the samples were obviously different, combining with the variation of microstructure characteristics of coal at high temperatures; the physical mechanism of damage and failure patterns of coal rock are explained from the viewpoint of energy.

1. Introduction

As a kind of inhomogeneous geological material, there are a large number of microfractures and microvoids inside the rock. The macroscopic failure of the rock results from microfractures' and microvoids' initiation, development, and interpenetration which eventually form the macroscopic crack. Under the high ground temperature environment conditions that the deep rock mass exists in, temperature plays an important role in the development and penetration of the microfractures and microvoids; and the variation of this microstructure is an irreversible, energy dissipation evolution process [1–4]. Analysis of energy transformation and conversion in the evolution of rock deformation and failure will contribute to reflecting the law of rock failure truly [5].

In recent years, more and more scholars began to study the physical mechanism of rock deformation and failure from the viewpoint of energy, and they have made a lot of valuable research results. Zhao and Xie [6] analyzed the rationality of using energy method to study the rock failure theoretically, the transformation process, and calculation principle as well as different failures to rock of the rock's elastic energy, plastic energy, surface energy, radiant energy, and kinetic energy in the process of rock deformation. They also studied the rock's energy dissipation and release in different deformation stages from the macro and micro perspectives. The study results showed that energy dissipation reduces the strength of rock, and energy release is the real reason for rock failure. Zhang and Gao [7] conducted uniaxial cyclic loading and unloading test on multiple sets of red sandstone specimens to calculate the internal size of various energy and obtained the evolution law of the elastic energy and dissipation energy which change with the axial stress. Yang et al. [8] conducted conventional triaxial compression test on marbles by using servo-control

testing machine. Based on these test results, they studied the rock sample's triaxial compression deformation failure and its energy characteristics. Results are as follows: the rock failure strain energy increases with the increase of confining pressure, and the relationship between them is positive linear; with the increase of confining pressure, all fracture energies of the rock increase in positive linear relationship. From the viewpoint of nonequilibrium thermodynamics, Xu et al. [9] combined the uniaxial compression and acoustic emission test of the rock exposed to high temperatures, expounded the characteristics of acoustic emission in evolution of rock deformation and failure, and analyzed the relationship between the strength of the rock exposed to high temperatures and the energy dissipation and energy release.

In addition to the temperature influence, the deep rock mass is inevitably influenced by high stress and dynamic disturbances in the process of mining and drilling such as rock burst, blasting caving, machine drilling, and the high order paragraphs mine. Therefore, in fact, the deep rock mass is in the effect of temperature, static pressure, and dynamic load. Under the dynamic load condition, the rock will show different physical and mechanical properties. Domestic and foreign scholars have made some studies in energy dissipation of the rock impact damage. Li and Gu [10] analyzed the difference in the rock's energy dissipation under different loading waveforms and explored the theory of rock's energy dissipation under different loading waves. According to the recurrence relations between the law of energy dissipation in rock and the brittle dynamic fracture criterion and the rock brittleness failure parameters and fragmentation under the action of shock loading, Hu et al. [11] obtained the relation among the impact energy, rock failure, and fragmentation distribution. Yong et al. [12] used optical microscope to observe the profile failure features of loading failure samples in dynamic tension form and static stretching form and found that the energy dissipation of stretch damage is related with rock failure closely. And Xia et al. [13] held the view that energy dissipation of the rock is affected by many factors such as rock porosity, lithology, the particle size of the rock, degree of consolidation of the rock, and fluid saturation degree. They analyzed the effect of porosity on impacting and damaging rock energy dissipation and the condition of energy dissipation when the rock suffers from critical damage.

In conclusion, in the study of characteristics of rock mechanics which belongs to deep rock mass engineering, most studies on mechanical properties of rock exposed to high temperatures are limited to the study of statics. However, in the study of characteristics of rock dynamic damage, it is simply believed that rock only suffers from dynamic load, and the influence of the deep high ground temperature on the internal structure of the rock is ignored. Some scholars have carried out rock dynamic experiments which consider the effect of temperature, but they never carried out the study from the view of impact damage and energy dissipation [14, 15]. These studies always focused on hard rock, and the study on low intensity soft rock is obviously inadequate. As the basic energy and important raw material, coal resource occupies an important strategic position in national economy. Compared with other hard rocks, coal has the features of small sturdiness coefficient, high porosity, and low compressive strength, and coal also has large difference in physical and mechanical properties with hard rock. When the coal and rock mass contact, the coal will present different mechanical properties. Therefore, it is particularly important to study the characteristics of impact mechanics of coal rock exposed to high temperatures.

In this article, the uniaxial dynamic compression experiment on coal rock exposed to high temperatures was carried out by using a split Hopkinson pressure bar (SHPB) system. The relationship between energy and time history under different temperature conditions was obtained. This paper analyzes the evolution of energy which changes with temperatures in the process of deformation and failure by combining the variation of microstructure characteristics of coal at high temperatures. It analyzes and discusses failure modes and broken blocks of the coal rock samples exposed to different temperatures, and the physical mechanism of damage and failure patterns of coal rock are explained from the viewpoint of energy.

2. SHPB Experiment on Coal Rock Exposed to High Temperatures

2.1. Preparation of Coal Rock Specimens. Coal rock is a kind of typical soft rock. There are various weak planes inside the raw coal such as cracks and voids. Artificial samples are different in internal structure, which leads to a great difference in mechanical parameter discreteness obtained by the test. For this reason, this experiment adopted the model material (consists of white cement, coal particles, and water) that has similar properties to coal rock in brittleness and dilatancy to make model samples which are similar to coal rock model samples. Volume ratio of the taken model material is as follows: cement : coal particles : water = 1 : 3 : 1; coal particles are the particles of grinding raw coal obtained through the 1 mm diameter sieve. In accordance with the requirement of dynamic loading test, the samples' length to diameter ratio is 1 : 1; cut a 50 mm diameter long plastic pipe into 50 mm long cylinders; inject ingredients into the short cylinder with grease smearing its inner surface, with iron wire tamping and floating on both ends; after 12 hours' maintenance, the mould release will be conducted; after demoulding, flatness of the sample's surface and ends will be checked, and the uneven ends will be polished to guarantee the smoothness of the sample to meet the test requirement; the samples after demoulding will be put into running water for 28 days, and the coal rock samples for test will be obtained. Figure 1 shows the representative finished samples of coal rock; their physical and mechanical properties under static load are shown in Table 1.

2.2. SHPB System. The dynamic impact loading test of coal rock was carried out by the SHPB system with a diameter of 50 mm which belongs to School of Resources and Safety Engineering in Central South University. In the SHPB system, the power system includes gas gun and emitting chamber; the loading system consists of special-shaped punch, the incident bar, transmission bar, and absorption bar which are made

Table 1: Some physical and mechanical properties of coal rock under static load.

Sample	Density/ ($kg \cdot cm^{-3}$)	Speed of longitudinal wave/($m \cdot s^{-1}$)	Elasticity modulus/ GPa	Deformation modulus/GPa	Peak stress/MPa	Peak strain/10^{-3}
Coal rock	1350	1895.5	0.410	0.649	5.136	13.725

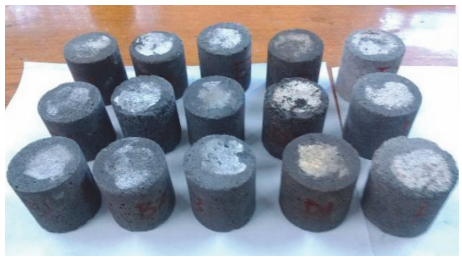

Figure 1: Physical maps of coal rock sample.

of high-strength 40 Cr alloy steel. The alloy steel has the features of 800 MPa ultimate strength, 5400 m/s ultrasonic wave velocity, and 7810 kg/m^3 density. The length of the incident bar, transmission bar, and absorption bar is 2000 mm, 1500 mm, and 500 mm, respectively; the diameter of them is 50 mm. SHPB system is shown in Figure 2. During the test, the rate of impact loading was controlled by adjusting the impact air pressure and the position of punch in emitting chamber. Under the action of air pressure, the punch hit against the incident bar and then produced one-dimensional stress wave. Because of the difference in sample and elastic bar wave impedance, a part of incident wave was transmitted across the sample, while a part of it was reflected back, and the last part was dissipated. By measuring voltage values of the strain gauge pasted on the two elastic bars, the sample's stress $\sigma(t)$, strain $\varepsilon(t)$, strain rate $\dot{\varepsilon}(t)$, and other mechanical parameters could be indirectly calculated. The calculation formulas [16] are

$$\begin{aligned} \sigma(t) &= \frac{A_0}{2A_S} E\left(\varepsilon_I + \varepsilon_R + \varepsilon_T\right), \\ \varepsilon(t) &= \frac{C_0}{L_S} \int_0^t \left(\varepsilon_I - \varepsilon_R - \varepsilon_T\right) dt, \\ \dot{\varepsilon}(t) &= \frac{C_0}{L_S} \left(\varepsilon_I - \varepsilon_R - \varepsilon_T\right). \end{aligned} \tag{1}$$

In the formula, A_0 and A_S are the cross-sectional areas of the sample and pressure bar; E is the elastic modulus of pressure bar; C_0 and L_S are the ultrasonic wave and the length of pressure bar; ε_I, ε_R, and ε_T are the incident strain, reflection strain, and transmission strain.

2.3. Test Methods and Procedures. Before the test, all samples were numbered and grouped according to different temperature levels. Test was divided into six temperature grades: 25, 100, 200, 300, 400, and 500°C. Under the condition of keeping temperature as the only variation, there were contrast experiments which used six samples in one temperature level. Heating equipment used in the experiment is the high temperature box made in Changcheng electric furnace plant in Tianxin district in Changsha. This kind of high temperature box is composed of high temperature resistance furnace and temperature controller. The electric furnace has many features; for example, model is SX-4-10, rated power is 4 kW, and the highest temperature can reach 1050°C. Put the numbered samples in high temperature box to heat; in order to ensure the samples are heated evenly, the heat rate is kept at 3°C/min; temperature should be kept constantly for 3 hours when it reached the predetermined amount. In order to avoid the cold shock which might lead to sample fracture [17] in the cooling process, a relative low rate of cooling to normal temperature is needed in the furnace, and coal rock samples exposed to different temperatures will be obtained.

Test method is to install the prepared samples correctly; smear proper grease on the ends of the samples; ensure that the ends of the samples contact with the elastic bar well; strictly control the same impact pressure and stroke of punch to achieve the consistency of the exerted dynamic loading; and achieve that the dynamic impact of the same loading strain rate condition can be operated along the axial direction until the samples damage. At the same time, test signals are recorded by the super dynamic strain gauge automatically. Figure 3 shows the sketch of sample installation on the rod of SHPB.

3. Experiment Principle and Basis

3.1. Dynamic Force Balance Verification. The SHPB system of the rock has used the rectangle wave loading method which is similar to the metal for a long time. As a kind of brittle material, rock is far lower than metal in strength. Conventional rectangular wave load will produce larger wave oscillation and dispersion effect, and the test accuracy will be seriously affected. The low failure strain of the rock, high loading rate condition, and the damage before the samples fully reach balanced stress—all these factors lead to the uselessness of the test results [18]. In order to solve this problem, scholars at home and abroad have performed a long-term research, put forward a series of pulse shaping technologies, and obtained some achievements [19–21].

The experiment adopted the special-shaped punch loading technology which was put forward by Li et al. [22]. The technology effectively increased the time of the stress wave rising edge. The test system has the characteristic of adapting heterogeneous brittle material to load under middle and high strain rates. Spindle punch can achieve half sinusoidal stress wave loading of constant strain rate. Dynamic stress balance is the precondition of any effective SHPB experiment. Figure 4 shows the time-stress diagram of the typical

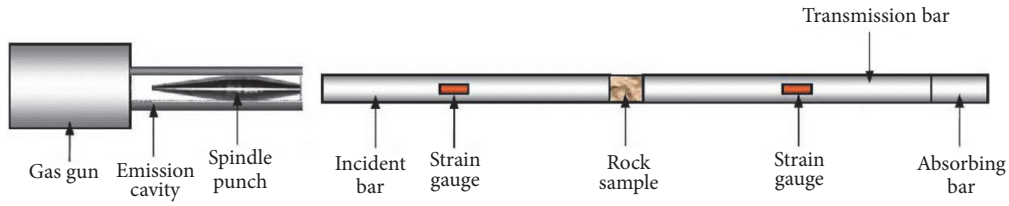

Figure 2: The functional diagram of SHPB.

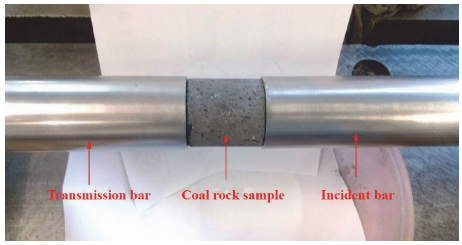

Figure 3: Sketch of sample installation.

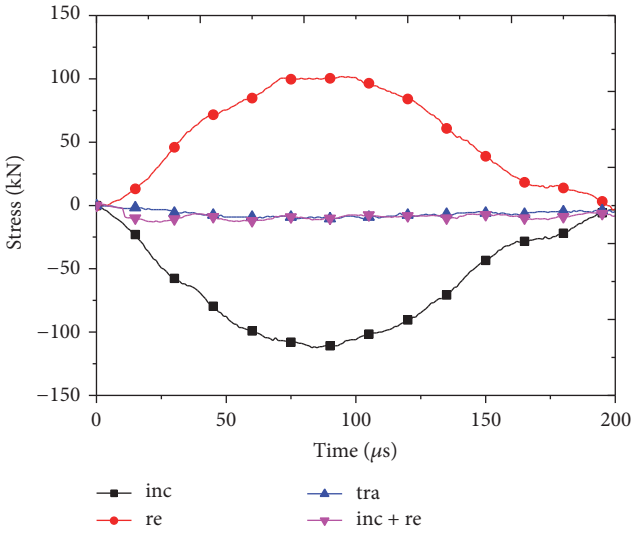

Figure 4: Dynamic force balance check for a typical test.

dynamic loading. Figure 4 shows that the superposition of the incident stress (inc), reflection stress (re), and the curve of transmission stress (tra) coincide, which indicates that both ends of the specimen reach dynamic force balance and there is a period of reflection platform in stress wave. It also suggests that the deformation and failure of the samples occur under constant strain rate.

3.2. Energy Distribution of the Sample Impact Failure. Based on one-dimensional stress wave theory and the law of conservation of energy, when incident bar is impacted by bullet, energy will propagate in elastic rod in the form of wave. Due to the difference in wave impedance of the sample and elastic bar, when the stress wave propagates to the contact surface of the elastic bar and sample, transmission and reflection will take place, and the remaining energy will be dissipated in the process of rock fragmentation. The incident energy, reflected energy, and transmission energy can be calculated through the incident stress $\sigma_I(t)$, reflection stress $\sigma_R(t)$, and transmission stress $\sigma_T(t)$ on the elastic bar:

$$E_I = \frac{A_0}{\rho_0 C_0} \int_0^\tau \sigma_I^2(t)\, dt,$$
$$E_R = \frac{A_0}{\rho_0 C_0} \int_0^\tau \sigma_R^2(t)\, dt, \quad (2)$$
$$E_T = \frac{A_0}{\rho_0 C_0} \int_0^\tau \sigma_T^2(t)\, dt.$$

In the formula, E_I, E_R, and E_T represent the incident energy, reflected energy, and transmission energy, respectively; $\sigma_I(t)$, $\sigma_R(t)$, and $\sigma_T(t)$ represent the incident stress, reflective stress, and transmission stress, respectively; A_0 and $\rho_0 C_0$ represent cross section area of the elastic bar and wave impedance, respectively; τ represents the duration of stress wave.

Due to the grease on both ends of the sample, fraction between the sample and the elastic bar can be negligible (that is to say, the energy loss can be ignored). In the evolution of sample impact damage, the total dissipation energy (E_L) can be represented as follows:

$$E_L = E_I - (E_R + E_T). \quad (3)$$

In the seventh formula, E_L is the dissipation energy in the evolution of sample failure and it includes the following several parts of energy [23, 24]: rock crushing energy, kinetic energy of fragments, and other dissipation energy, such as heat energy. Zhang et al. [25] measured the speed of rock fragments by high speed camera in SHPB experiment and pointed out that the rock crushing energy accounted for about 95% of the total energy and the remaining two kinds of energy were less than 5%; and we can approximate the absorbed energy of the sample equal to the total dissipation energy for rock breaking, which can be shown as $E_A = E_L$. In the process of impact failure, the value of SEA of unit volume rock samples is defined simultaneously as follows:

$$\mathrm{SEA} = \frac{E_A}{V_0}. \quad (4)$$

In the formula, SEA stands for the specific energy absorption value; V_0 stands for the sample volume.

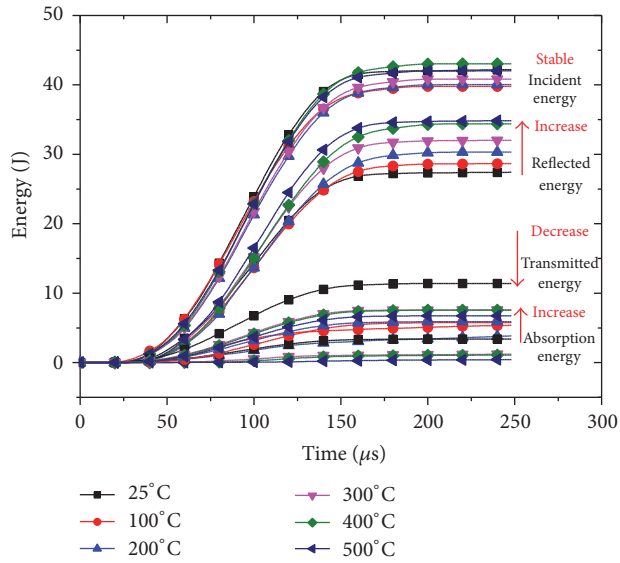

Figure 5: Time history curves of energy under impact loading.

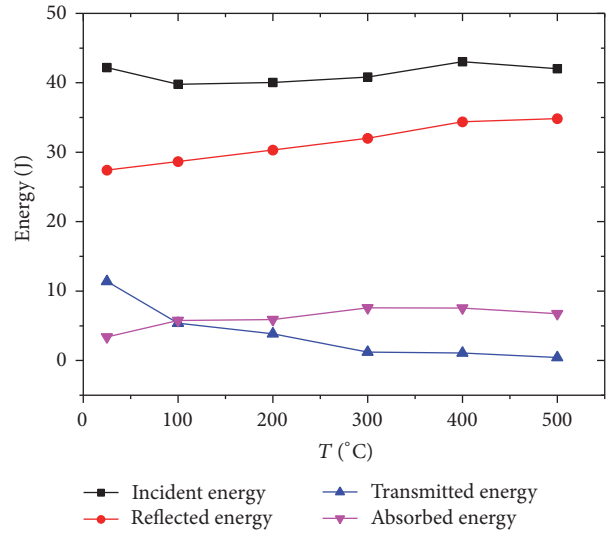

Figure 6: The evolution of energy at different temperatures.

4. Analysis and Discussion on the Test Results

Verify the results in the method of dynamic balance and eliminate the test data which is unable to achieve the stress balance. According to the above-mentioned energy calculation formulas from the fourth to the eighth, the incident energy, reflected energy, transmission energy, absorbed energy, and the values of SEA of the coal rock exposed to high temperatures will be calculated, respectively. Table 2 shows the variation of energy with temperatures during the experimental process.

4.1. Variation of Energy during the Process of Impact Failure. During the process of dynamic loading, the stress wave duration has a certain effect on impact breaking and dissipation of the rock [26]. In order to analyze the evolution of energy with time during the dynamic loading process of the sample, Figure 5 shows the energy-time curves under different temperature conditions. Figure 5 shows that, in the initial loading stage, all energies increase rapidly with the increase of stress wave duration; when loading time reaches about 150 μs, the growth rate slows down rapidly and the energy is close to the maximum. Under the same loading condition, the incident energy of the system is equal; reflected energy occupies the largest proportion and surpasses more than 60% of the total incident energy; the value of transmitted energy and absorbed energy is small. With the increase of temperature, reflected energy and absorbed energy show the increasing trends, and transmitted energy continues to reduce.

In order to further analyze the effect of temperature on energy dissipation, Figure 6 shows the evolution curve of energy with temperature during the impact loading process. It can be seen that when samples are in normal states, the reflected energy is 27.41 J, which accounts for 65% of the total incident energy; the amount by which transmitted energy exceeds absorbed energy is 11.39 J and 3.4 J, which accounts for 27% and 8% of the total incident energy. With the increase of temperature, the reflected energy increases continuously; transmitted energy and absorbed energy show an opposite variation. At the temperature of 25 to 100°C, transmitted energy quickly reduces, while the absorbed energy quickly increases. After 100°C, absorbed energy is more than transmitted energy and the surplus value is 5.76 J and 5.37 J, which accounts for 14.4% and 13.4% of the total incident energy. And then the variations of absorbed energy and transmitted energy slow down with temperature. When temperature reaches 500°C, reflected energy increases to 34.85 J and accounts for 83% of the total incident energy; absorbed energy increases to 6.75 J and accounts for 16% of the total incident energy, while the value of the transmitted energy is only 0.42 J, accounting for 1% of the total incident energy.

The reasons for the energy change are the following: there are lots of cracks and voids inside the coal rock samples, which leads to the low density, and the wave impedance is far less than the elastic wave impedance. When incident wave reaches the boundary of the sample and elastic rod, most incident wave will be reflected back, which also is a main reason why reflected energy accounts for more than 60% of the incident energy. When heating samples from room temperature to 100°C, the moisture inside the samples will evaporate into steam. The escape of steam leads to expansion of the original cracks and decrease of the samples' density, which leads to the sample wave impedance reduction, reflectance of stress wave increase, and transmittance of stress wave decrease. At the same time, new cracks and a large number of defect surfaces involved in the process of energy dissipation make absorbed energy of samples increase quickly. When the temperature exceeds 100°C, moisture inside samples is completely lost; mineral grains expand when heated. Due to the different thermal expansion coefficients among particles, structure thermal stress will be produced in samples, which will compress cracks, decrease fractures and improve the contact relationship between mineral grains, and slow down the declining rate of coal rock wave impedance, and the performance is the slow variation of energy with temperature.

Table 2: The variation of energy with temperature during the experimental process.

T/°C	Sample number	Incident energy E_I/J	Reflected energy E_R/J	Transmitted energy E_T/J	Absorbed energy E_A/J	SEA /J·cm^{-3}
25 (normal temperature)	A1	38.77	25.28	10.37	3.12	0.0406
	A3	43.52	28.30	11.79	3.43	0.0438
	A4	39.86	25.88	10.83	3.15	0.0384
	A5	46.65	30.18	12.57	3.90	0.0491
	Average value	42.20	27.41	11.39	3.40	0.0430
100	B1	40.12	28.86	5.42	5.84	0.0710
	B2	39.66	28.58	5.26	5.82	0.0713
	B3	41.23	29.69	5.57	5.97	0.0687
	B6	38.15	27.51	5.23	5.41	0.0639
	Average value	39.79	28.66	5.37	5.76	0.0687
200	C2	38.78	29.51	3.59	5.68	0.0681
	C4	41.23	31.45	3.86	5.92	0.0709
	C5	39.69	30.16	3.92	5.61	0.0711
	C6	40.46	30.12	3.99	6.35	0.0780
	Average value	40.04	30.31	3.84	5.89	0.0720
300	D1	42.11	32.85	1.35	7.91	0.0957
	D2	39.76	31.23	1.17	7.36	0.0882
	D3	43.03	33.56	1.29	8.18	0.1016
	D5	38.46	30.44	1.07	6.95	0.0820
	Average value	40.84	32.02	1.22	7.60	0.0917
400	E1	43.43	34.76	1.08	7.59	0.0916
	E3	42.17	33.64	1.05	7.48	0.0923
	E4	41.88	33.51	1.04	7.33	0.0854
	E5	44.68	35.69	1.15	7.84	0.0938
	Average value	43.04	34.40	1.08	7.56	0.0907
500	F3	41.26	34.18	0.39	6.69	0.0828
	F4	43.15	35.83	0.47	6.85	0.0884
	F5	40.87	34.04	0.38	6.45	0.0756
	F6	42.80	35.35	0.44	7.01	0.0851
	Average value	42.02	34.85	0.42	6.75	0.0828

4.2. Energy Dissipation Rate. The whole failure process of coal rock sample is accompanied by energy dissipation and loss; the actual energy used for rock breaking accounts for a small proportion. Rock samples belong to nonhomogeneous material, especially the coal rock. There are many defects inside the coal rock samples, such as microcracks, cracks, voids, and the difference in density and wave impedance of rock samples and elastic rod, which make energy that transfers between the elastic bar and rock samples in the form of wave decompose into reflected energy (wave passes different dielectric interfaces and forms reflected wave; this kind of energy exists in the form of reflected wave); transmitted energy (wave passes the rock samples and forms transmitted wave; this kind of energy exists in the form of transmitted wave); absorbed energy (in the process of passing rock samples, this kind of energy is used for rock breaking); and other dissipated energies (such as energy dissipated in the fraction between the sample and the bar). With grease on both ends of the samples, this paper holds that other energy dissipation is very small; there is no need to consider the loss of the energy and take the seventh formula to describe absorbed energy. By calculating the ratio of energy

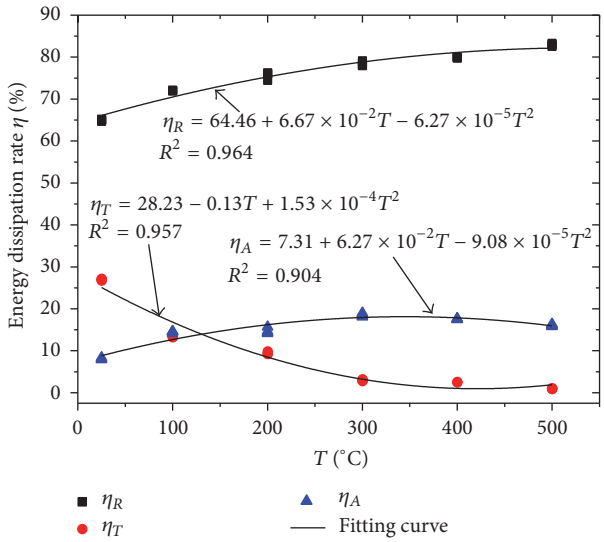

Figure 7: The variation of energy dissipation rate with temperatures.

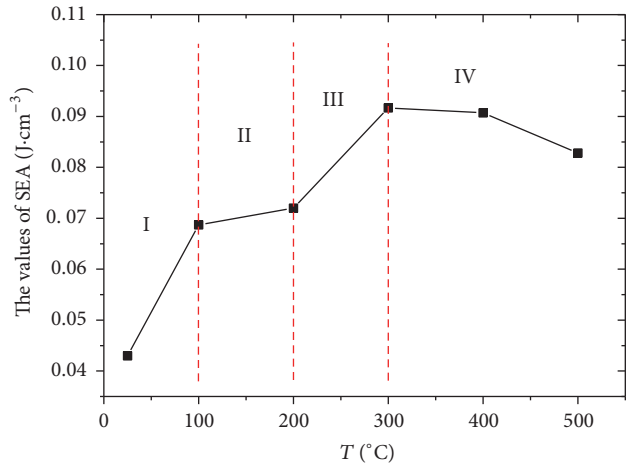

Figure 8: The relation between the values of SEA and temperature.

accounting for the total incident energy, Figure 7 shows the variation of energy dissipation rate with the temperatures.

As shown in Figure 7, before 400°C, both energy reflectivity and absorptivity are on the rise; after 400°C, energy reflectivity continues to rise, while the absorption rate decreases, and energy transmission rate decreases in the whole experiment temperature range, and the energy reflectivity is far greater than the other two energy dissipation rates. Under normal temperature, energy reflectivity has reached 65%; when the temperature is 500°C, energy reflectivity reaches 83% and occupies the main part. During the experiment, the coal rock samples contain cement, coal particles, water, and air at the same time, which leads to different medium within the rock mass. The sample is poor in density because many microcracks and microvoids exist within the internals. Bar and samples are also different in density and wave impedance. A large number of medium interfaces allow that most of incident wave in the process of propagation reflects back to the incident ends and most of energy dissipates in the form of reflection wave; thus reflectivity accounts for most of the proportion of the energy. With the increase of temperature, the expansion of the coal rock internal primary cracks and voids, and the production of new cracks, more and more interfaces are produced and energy reflectance increases gradually. When the temperature reaches 500°C, energy reflectance has been as high as 83%. With the increase of temperature and the difference in thermal expansion coefficient between particles, the number of cracks and voids inside the samples is still increasing, although there are a few primary cracks and voids closed. In order to make the macro failure of the coal rock samples occur, more cracks and voids need to participate, so coal rock samples need to absorb more energy and then energy absorption rate increases. After 400°C, coal rock samples have been destroyed; with the increase of temperature, only a little energy can make the sample suffer failure and then energy absorption rate reduces.

In order to get the quantitative relationship between energy dissipation rate and temperatures, quadratic function is used to fit the experimental data. The simulated formulas are as follows:

$$\eta_R = 64.46 + 6.67 \times 10^{-2}T - 6.27 \times 10^{-5}T^2,$$
$$\eta_T = 28.23 - 0.13T + 1.53 \times 10^{-4}T^2, \quad (5)$$
$$\eta_A = 7.31 + 6.27 \times 10^{-2}T - 9.08 \times 10^{-5}T^2.$$

The above simulated formulas could describe well the evolution of energy dissipation and temperatures at the range of normal temperature of 500°C.

4.3. The Relation between the Value of SEA and Temperature. The amount of sample's internal cracks and the superficial area of sample's failure can be directly represented by the amount of rock's absorbed energy. Figure 8 shows the evolution curve between the values of SEA of the coal rock samples and temperatures. The figure shows that, under the condition of different temperatures, the values of SEA of the coal rock samples are between 0.04 J·cm^{-3} and 0.1 J·cm^{-3}, and with the increase of temperature, the evolution can be divided into four different stages. In the first phase, at the temperature of 25 to 100°C the values of SEA increase from 0.043 J·cm^{-3} to 0.069 J·cm^{-3} rapidly, and the increase rate is 60%. The main reason for the increase of the values of SEA in this stage is the increase of cracks and failure's superficial area caused by the moisture evaporation inside the samples and the increase of porosity. In the second phase, at the temperature of 100 to 200°C, the increase rate of the values of SEA significantly decreases; the values of SEA increase from 0.069 J·cm^{-3} to 0.072 J·cm^{-3}, and the growth rate is only 3%; this is because the thermal expansion coefficient of mineral grains is different which makes structure thermal stress inside the samples play the leading role and the contact relationship between particles gets improved and cracks close, thus inhibiting the absorption of energy. In the third stage, at the temperature of 200 to 300°C, the values of SEA increase from 0.072 J·cm^{-3}

to 0.092 J·cm^{-3}, with a growth rate of 28%. The main reason for the increase of the absorbed energy is that, under high temperatures, mineral particles swell rapidly and the effect of structure thermal stress is no longer obvious, with some new cracks. And at this stage of high temperature some organic matter within the coal rock gradually decomposes into pyrolysis gas, and the generation of pyrolysis gas once again leads to expansion of the cracks inside the samples and increase of the damage. In the fourth stage, at the temperature of 300 to 500°C, the values of SEA no longer continue to increase with temperatures but appear to have a downward trend; they decrease from 0.092 J·cm^{-3} to 0.083 J·cm^{-3}, with a decrease rate of 9.8%. The main reason for this phenomenon is that under high temperature mechanical properties of coal rock samples produce serious degradation. In this phase, thermal decomposition and thermal deformation of mineral composition play the leading roles, and the samples become very loose. In the process of loading, little energy is needed to make samples suffer from crushing failure, and wave impedance of the samples is very small. Energy at this stage mainly is reflected off instead of using to break the rock.

4.4. Failure Patterns and Mechanism of Coal Rock Sample. Fracture and failure of the rock under shock loading is actually a process of energy absorption and dissipation. Study on the evolution of failure patterns of the coal rock exposed to high temperatures is advantageous to analyze the influence of temperature and energy absorption on its failure modes. As shown in Figure 9, from the point of broken form, with the increase of temperature, main failure modes of the samples get changed: the size of fragments reduces greatly and becomes more homogeneous; the amount of powder particles increases; temperature effect is shown obviously. At the temperature of 25 to 200°C, there is a chunk which is equal to the sample in length after failure, accompanied by some strip cylinders at the same time; at this stage the main failure mode is tensile fracture; although temperature effect produces a certain amount of failure, due to the structure thermal stress effect, the sample keeps in perfect condition basically and the surface defects and energy absorption are less, and then fewer powder particles are produced at this stage. When temperature reaches 300°C, the samples are damaged into several homogeneous conical fragments; the size of broken blocks significantly reduces and the amount of powder particles increases. At this phase, the effect of structure thermal stress becomes weak, and thermal damage increases; the sample absorbs more energy in the process of impact loading; at the same time due to the decrease of sample's strength, end effect is apparent, which causes shear failure of the sample. At the temperature of 400°C, the coal rock still has a certain strength; however, under high temperature, the internal cracks develop well and thermal damage becomes large and samples become very loose; under this condition, only by absorbing little energy can the whole sample structure occur in an overall broken situation characterized by homogeneous grain fragments. At the temperature of 500°C, thermal damage plays a leading role in the failure of the sample; the sample can be damaged into homogeneous powder particles even if absorbing little energy.

5. Discussion

It is well known to us that there is energy dissipation in the process of wave propagation in the bar and sample. And the bar is a kind of dense homogeneous material; little energy will be lost in the wave propagation in the bar. Other energy dissipation (η_O) mainly is the energy dissipation produced by fraction between the sample and the bar, and the amount is little. Many scholars hold that the amount can be negligible. However, which degree does the amount reach in the experiment and can it be neglected really? Through the description of energy dissipation rate and use of the quadratic function fitting to quantify the energy dissipation rate, then we can find out the evolution of energy dissipation rate with temperature which is controlled at the room temperature of 500°C. Fitting curve is of high reliability, and the reliability coefficient is greater than 0.9.

To quantify the other energy dissipation rate, this paper calculated the values of other energy dissipation rates with temperature which is controlled at 25 to 500°C by means of mathematical inversion method and then described the other energy dissipation rate. Inversion formula is as follows:

$$100\% = \eta_A + \eta_R + \eta_T + \eta_O. \tag{6}$$

In the formula, η_A represents energy absorption rate; η_R represents energy reflection rate; η_T represents energy transmission rate; η_O represents other energy dissipation rates. Change the form of the twelfth formula, and the calculation formula of the other energy dissipation rate can be obtained, which is as follows:

$$\eta_O = 100\% - (\eta_A + \eta_R + \eta_T). \tag{7}$$

Figure 10 shows the evolution of the other energy dissipation rate with temperature, which is calculated by the means of inversion. From the figure, we can easily notice that the other energy dissipation rate is really small; the minimum is 0.195%, and the largest one is only 0.605%. The great changes of both ends of the sample with the increase of temperature can be reflected indirectly, although the other energy dissipation rate is small. Under normal temperature, both ends and surface of the sample are rough and surface has no obvious cracks; in the experiment, fraction and other factors dissipate little energy; that is to say, the other energy dissipation rate is the minimal. When the temperature increases to 500°C, water vapor overflows and thermal stress makes the microcracks and voids expand to generate cracks in surface. Mineral grains have different thermal expansion coefficients, which makes the ends of the sample seriously uneven. All these factors make the fraction between the sample and bar increase. Thus at the temperature of 500°C, the other energy dissipation rate is the largest.

6. Conclusion

The energy dissipation characteristics in the process of impact failure of coal rock exposed to high temperatures were studied by using a split Hopkinson pressure bar (SHPB) system. The evolution of energy with temperature during the experimental process was explored. Combining thermal damage

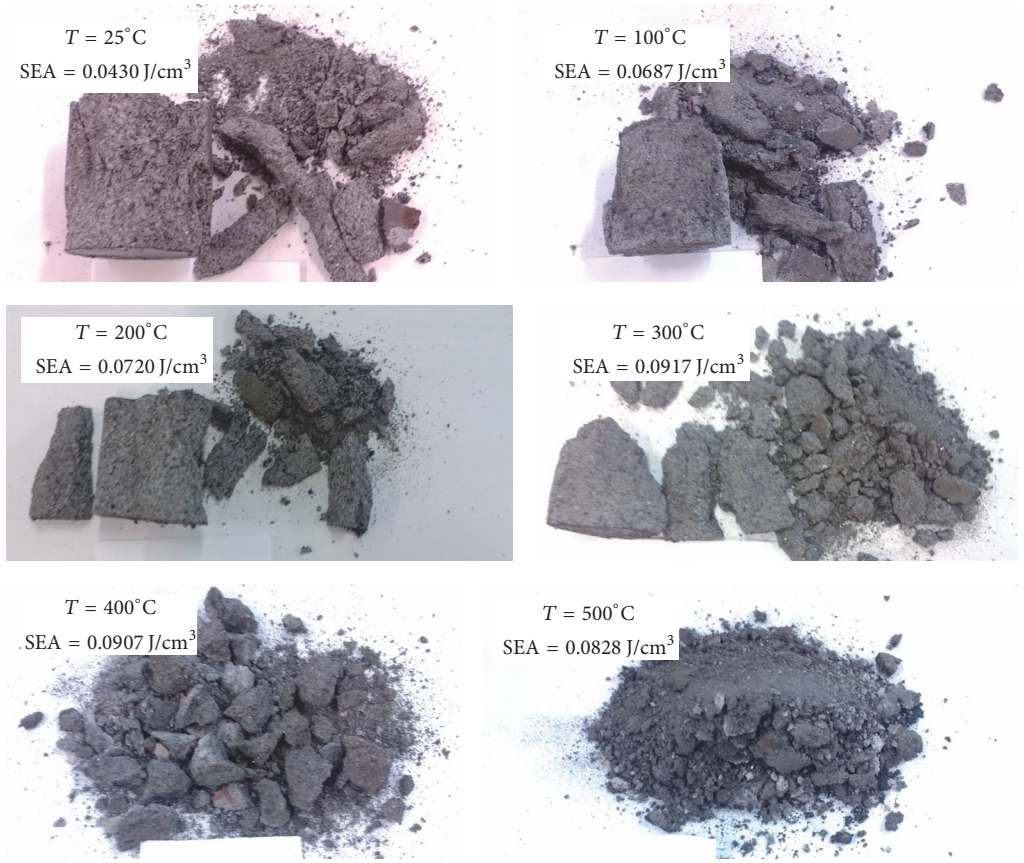

Figure 9: Failure patterns of coal rock under different temperatures.

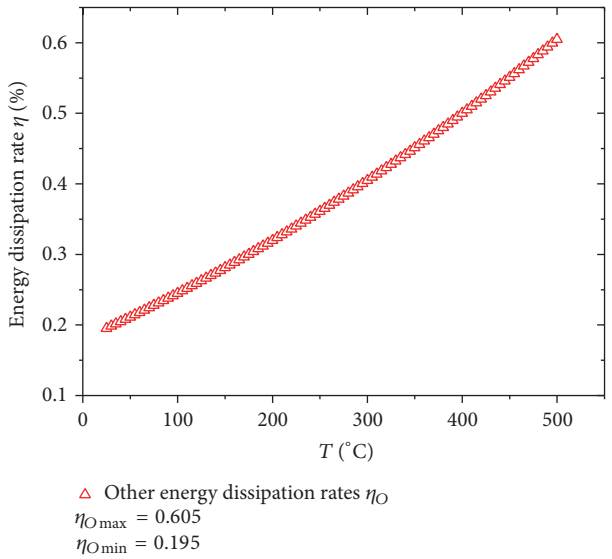

Figure 10: The relationship between other energy dispassion rates and temperature.

theory and energy dissipation theory, this paper analyzes the failure patterns and internal mechanism of coal rock under different temperatures. The following conclusions are obtained.

(1) Due to the small wave impedance of coal rock, in the process of impact loading, more than 60% of the incident energy is not involved in the breaking of the sample, while it is reflected off; and with the increase of temperature the reflection energy continues to increase; at the temperature of 500°C, energy reflectivity reaches 83%.

(2) During the period of low temperature, the absorbed energy of the sample is less than the transmitted energy; with the increase of temperature, transmitted energy and absorbed energy show an opposite variation: absorbed energy increases, while transmitted energy reduces; the absorbed energy is greater than the transmitted energy after 100°C.

(3) The amount of the sample's internal cracks and the superficial area of the sample's failure can be directly represented by the values of SEA. Evaporation of free water, expansion of mineral particles, structure thermal stress, and pyrolysis gas produced by decomposition of organic matter are the important factors that lead to the failure evolution of coal rock. Under different temperature conditions, the leading role is played by different factors, which make the evolution of the values of SEA with temperature divide into four stages.

(4) Under different temperature conditions, failure modes and broken blocks of the coal rock samples are obviously different. At the stage of low temperature, the samples are characterized by tensile failure and shear failure; the higher the values of SEA, the smaller the broken blocks and the more the powder particles. Under the condition of high temperature, thermal damage plays a leading role in rock failure, and the sample degrades seriously. The sample will break into homogeneous fragments and powder particles even if it absorbs little energy.

Competing Interests

The authors declare no conflict of interests.

Acknowledgments

This work is financially supported by the Research Fund of the State Key Laboratory of Coal Mine Disaster Dynamics and Control; National Natural Science Foundation of China (51304241, 51504044); China Postdoctoral Science Foundation (2014M552164, 2015M570607); Doctoral Foundation of the Ministry of Education of China (20130162120015); and the Research Fund of Chongqing Basic Science and Cutting-Edge Technology Special Projects (cstc2016jcyjA1861).

References

[1] H.-P. Xie, R.-D. Peng, and Y. Ju, "Energy dissipation of rock deformation and fracture," *Chinese Journal of Rock Mechanics and Engineering*, vol. 23, no. 21, pp. 3565–3570, 2004.

[2] T.-B. Yin, X.-B. Li, Z.-Y. Ye, F.-Q. Gong, and Z.-L. Zhou, "Energy dissipation of rock fracture under thermo-mechanical coupling and dynamic disturbances," *Chinese Journal of Rock Mechanics and Engineering*, vol. 32, no. 6, pp. 1197–1202, 2013.

[3] Z.-Z. Zhang, F. Gao, and X.-L. Xu, "Experimental study of temperature effect of mechanical properties of granite," *Rock and Soil Mechanics*, vol. 32, no. 8, pp. 2346–2352, 2011.

[4] S. Liu, J.-Y. Xu, Z.-Q. Liu, L.-P. Zhi, and T.-F. Chen, "Temperature effect on strength and damage property of rock mass," *Journal of Mining & Safety Engineering*, vol. 30, no. 4, pp. 583–588, 2013.

[5] Y. Ming-Qing and H. An-Zeng, "Energy analysis of the process of rock sample destruction," *Chinese Journal of Rock Mechanics and Engineering*, vol. 21, no. 6, pp. 778–781, 2004.

[6] Z.-H. Zhao and H.-P. Xie, "Energy transfer and energy dissipation in rock deformation and fracture," *Journal of Sichuan University*, vol. 40, no. 2, pp. 26–31, 2008.

[7] Z.-Z. Zhang and F. Gao, "Experimental research on energy evolution of red sandstone samples under uniaxial compression," *Chinese Journal of Rock Mechanics and Engineering*, vol. 31, no. 5, pp. 953–962, 2012.

[8] S.-Q. Yang, W.-Y. Xu, and C.-D. Su, "Study on the deformation failure and energy properties of marble specimen under triaxial compression," *Engineering Mechanics*, vol. 24, no. 1, pp. 136–142, 2007.

[9] X.-L. Xu, F. Gao, Q. Zhou, and J. Chen, "Energy analysis of rock deformation and failure process after high temperature," *Journal of Wuhan University of Technology*, vol. 33, no. 1, pp. 104–107, 2011.

[10] X. Li and D. Gu, "Energy dissipation of rock under impulsive loading with different waveforms," *Explosion and Shock Waves*, vol. 14, no. 2, pp. 129–139, 1994.

[11] L.-Q. Hu, X.-B. Li, and F.-J. Zhao, "Study on energy consumption in fracture and damage of rock induced by impact loadings," *Chinese Journal of Rock Mechanics and Engineering*, vol. 21, supplement 2, pp. 2304–2308, 2002.

[12] Y. Yong, Z. Zongxian, Y. Jie, and L. Guohua, "Energy dissipation and damage characters in rock direct tensile destruction," *Chinese Journal of Rock Mechanics and Engineering*, vol. 17, no. 4, pp. 386–392, 1998.

[13] C.-J. Xia, H.-P. Xie, Y. Ju, and H.-W. Zhou, "Experimental study of energy dissipation of porous rock under impact loading," *Engineering Mechanics*, vol. 23, no. 9, pp. 1–5, 2006.

[14] Z. Zong-Xian, Y. Jie, J. Lin-Ge, and Y. Yong, "Experimental study on dynamic Fracture of rock under condition of high temperature heating," *Nonferrous Metals*, no. 1, pp. 1–3, 1999.

[15] L.-P. Zhi, J.-Y. Xu, Z.-Q. Liu, S. Liu, and T.-F. Chen, "Research on impacting failure behavior and fluctuation characteristics of granite exposed to high temperature," *Chinese Journal of Rock Mechanics and Engineering*, vol. 32, no. 1, pp. 135–142, 2013.

[16] T.-B. Yin, X.-B. Li, B. Wang, Z.-Q. Yin, and J.-F. Jin, "Mechanical properties of sandstones after high temperature under dynamic loading," *Chinese Journal of Geotechnical Engineering*, vol. 33, no. 5, pp. 777–784, 2011.

[17] M. H. B. Nasseri, A. Schubnel, and R. P. Young, "Coupled evolutions of fracture toughness and elastic wave velocities at high crack density in thermally treated Westerly granite," *International Journal of Rock Mechanics and Mining Sciences*, vol. 44, no. 4, pp. 601–616, 2007.

[18] L. Xi-Bing, *Rock Dynamics Fundamentals and Applications* , Science Press, Beijing, China, 2014.

[19] D. J. Frew, M. J. Forrestal, and W. Chen, "Pulse shaping techniques for testing brittle materials with a split Hopkinson pressure bar," *Experimental Mechanics*, vol. 42, no. 1, pp. 93–106, 2002.

[20] D. J. Parry, A. G. Walker, and P. R. Dixon, "Hopkinson bar pulse smoothing," *Measurement Science & Technology*, vol. 6, no. 5, pp. 443–446, 1995.

[21] R. J. Christensen, S. R. Swanson, and W. S. Brown, "Split-hopkinson-bar tests on rock under confining pressure," *Experimental Mechanics*, vol. 12, no. 11, pp. 508–513, 1972.

[22] X. B. Li, T. S. Lok, J. Zhao, and P. J. Zhao, "Oscillation elimination in the Hopkinson bar apparatus and resultant complete dynamic stress-strain curves for rocks," *International Journal of Rock Mechanics and Mining Sciences*, vol. 37, no. 7, pp. 1055–1060, 2000.

[23] L. Ming, *Research on Rupture Mechanisms of Coal Measures Sandstone under High Temperature and Impact Load*, China University of Mining and Technology, 2014.

[24] Y. Guang-Zhi, Z. Dong-Ming, D. Gao-Fei, and W. Lin, "Damage model of rock and the damage energy index of rockburst," *Journal of Chongqing University*, vol. 25, no. 9, pp. 75–78, 2002.

[25] Z. X. Zhang, S. Q. Kou, J. Yu, Y. Yu, L. G. Jiang, and P.-A. Lindqvist, "Effects of loading rate on rock fracture," *International Journal of Rock Mechanics and Mining Sciences*, vol. 36, no. 5, pp. 597–611, 1999.

[26] L. Hong, Z.-L. Zhou, T.-B. Yin, G.-Y. Liao, and Z.-Y. Ye, "Energy consumption in rock fragmentation at intermediate strain rate," *Journal of Central South University of Technology*, vol. 16, no. 4, pp. 677–682, 2009.